ADVANCES IN FORESTRY SCIENCE

OPEN ACCESS

Prediction of dendrometric variables by optical data in *Pinus taeda* L. stand

Carla Talita Pertille[1*] *Marcos Felipe Nicoletti*[2] *Larissa Regina Topanotti*[3] *Luís Paulo Baldiserra Schorr*[4]

[1]Universidade do Estado de Santa Catarina, Av. Luis de Camões, 2090, Conta Dinheiro, CEP 88520-000, Lages, SC, Brasil
[2]Universidade do Estado de Santa Catarina, Av. Luis de Camões, 2090, Conta Dinheiro, CEP 88520-000, Lages, SC, Brasil
[3]Universidade Federal de Santa Catarina, Rod. Ulysses Gaboardi, CEP 89520-000, Curitibanos, SC, Brasil
[4]Universidade Federal de Lavras, Caixa Postal 3037, CEP 37200-000, Lavras, MG, Brasil

Original Article

***Corresponding author:**
carlatpertille@gmail.com

Keywords:
Remote Sensing

Vegetation index

Forest management

Palavras-chave:
Sensoriamento Remoto

Índices de vegetação

Manejo florestal

Received in
2020/02/25

Accepted on
2021/07/07

Published in
2021/08/31

DOI: http://dx.doi.org/10.34062/afs.v8i2.9875

ABSTRACT: The objective of this work was to estimate the basal area and volume of a *Pinus taeda* L. stands located in Santa Catarina, using data from an orbital image of the Landsat-8/OLI sensor. In this sense, a forest research was carried out, with a random sampling process using the fixed area method. 20 circular parcels of 400 m² were allocated. An orbital image of the Landsat-8/OLI sensor was used and 10 average vegetation indices per plot were calculated. These were correlated as variables of volume and basal area per plot, decorative by the forest inventory. The index with the best correlation for the volume was GNDVI with 0.47 and for a basal area, the MVI with 0.51. The adjustment of the regression models showed adjusted R^2 indices of 0.5639 and Syx of 13.31% for volume, and 0.5213 and 11.93% for the basal area. It was possible to estimate the volume and basal area of the stands through the spectral data, however, it is recommended that this same technique be tested in other species of the genus Pinus spp. and with high spatial resolution media.

Predição de variáveis dendrométricas por dados ópticos em um povoamento de *Pinus taeda* L.

RESUMO: O objetivo desse trabalho foi estimar área basal e volume de um povoamento de *Pinus taeda* L. a partir de dados de imagem orbital do sensor Landsat-8/OLI. Para isso, foi realizado um inventário florestal, pelo método de área fixa e amostragem aleatória simples. Foram alocadas 20 parcelas circulares de 400 m². Foi utilizada uma imagem orbital do sensor Landsat-8/OLI e foram calculados 10 índices de vegetação médios por parcela. Esses índices foram correlacionados com as variáveis volume e área basal por parcela, obtidos pelo inventário florestal. O índice com a melhor correlação para o volume foi o Green Normalized Difference Vegetation Index (GNDVI) com 0,47 e para a área basal, o MVI, com 0,51. O ajuste dos modelos de regressão com esses índices apresentou R^2 ajustado de 0,5639 e Syx de 13,31% para o volume, e 0,5213 e 11,93% para a área basal. Foi possível estimar o volume e área basal do povoamento por meio dos dados espectrais, porém, recomenda-se que essa metodologia seja testada em outras espécies do gênero Pinus spp. e com sensores de média a alta resolução espacial.

Introduction

Dendrometric variables are important forest information and their monitoring is one of the main tasks of the regional forest management plans aimed at preserving the environment and strengthening the local economy (Stournara et al., 2017). The volume is one of these variables and one of the main structural attributes of the forest, as well as the diameter at breast height and basal area, obtained by forest inventory techniques and estimates using general allometric equations (Chinembiri et al., 2013; Gara et al., 2014).

However, forest inventory methods are costly, time-consuming, laborious, and limited in extent (Tesfamichael et al., 2010). Thus, the use of Remote Sensing techniques is increasing, allowing the obtaining of information from the inventoried areas using satellite images of medium and high spatial resolution, setting up a new scenario in the monitoring of a forest stand (Gunlu et al., 2014). One of the main advantages of orbital images is the ability to obtain spatial and temporal information about the variables of interest in large areas with relatively low cost (Zhang et al., 2014).

The estimation of forest parameters through orbital images includes the use of regression models that relate spectral responses of vegetation indices or bands with biophysical variables of the forest stand. In the image, the reflectance of the targets is characterized in each of the spectral bands or by the indices (Berra et al., 2012). According to Almeida et al. (2015), the indices highlight the antagonistic behavior of the vegetation in the spectral bands of red and near infrared, being more vulnerable the variations of the canopy structures than the individual bands.

Among the indexes available in the literature, the Normalized Difference Vegetation Index (NDVI) developed by Rouse et al. (1974) is the best known and used for vegetation characterization and monitoring studies. The Simple Ratio (SR) vegetation index is the oldest index, based on the ratio between the near infrared band and the red band (Jordan, 1969), while the Adjusted Vegetation Index for the Soil Adjusted Vegetation Index (SAVI), proposed by Huete (1988), is characterized by reducing the effects of background soil on the vegetation signal by incorporating a soil adjustment constant into the equation vegetation in orbital images.

In this sense, the use of images of medium spatial and temporal resolution becomes an attractive option for the estimation and the mapping of forest attributes. A sensor with these characteristics comprises the Landsat-8/OLI (Operational Land Imager) with free distribution of images, acquired 16 days apart and with better spectral capacity (Dube et al., 2015).

Several studies aimed at obtaining dendrometric variables have already been developed with this satellite, as can be mentioned: estimation of density of trees, basal area, volume and biomass data using Landsat/TM (Thematic Mapper) in northern Greece (Mallinis et al., 2004); Obtaining parameters of canopy cover, aboveground biomass, volume, Shannon diversity index and basal area using the Landsat Enhanced Thematic Mapper (ETM) bands and the normalized difference vegetation index transformed derivative (TNDVI) (Alrababah et al., 2011); development of wood volume estimator models from Landsat 5 TM images, based on regional forest inventory data (Berra et al., 2012), timber volume estimation of a stand of Pinus elliottii Engelm. integrating data from LISS-III/ ResourceSat-1 and Landsat 5/TM sensors (Berra et al., 2016) and wood volume estimation of a stand of Eucalyptus grandis using Landsat-8/OLI (Alba et al., 2017).

Therefore, the importance of accurate and direct estimates of forest stand characteristics, such as volume and basal area, can be obtained through the association of optical data and data from the forest inventory. In this scenario, this study aimed to estimate the basal area and volume of a *Pinus taeda* L. stand, using data from an orbital image of the Landsat-8/OLI sensor.

Material and Methods

Study area

The study was carried out in a stand of 43.10 hectares with 14 years old *Pinus taeda* L. located in the municipality of Caibi, west of the state of Santa Catarina (Figure 1). The planting was subjected to thinning at 8 and 12 years old. Located at an altitude of 337 meters, the area presents mesothermic climate of the humid type, according to Koeppen classification with frequent frosts in the months of June and July. The average temperature of the municipality is 19,6º and the annual precipitation is between 1900 mm and 2000 mm (Alvares et al., 2013).

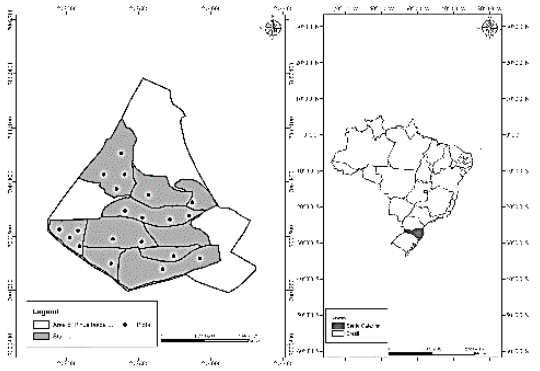

Figure 1. Location of the study area: Brazil, Santa Catarina and area of *Pinus taeda* L.

The forest inventory procedure was performed using the fixed area sampling method and simple random sampling process. Ten plots were

installed circular of 400 m² and radius of 11.28 meters. The circumference at 1,3 m height (CAP) of all trees in the plot was measured with a tape measure and the height of dominant trees according to Assmann's concept (1970) were measured using the Easy Measure computational application. The geographic position of the plots was obtained with the View Ranger application whose data were georeferenced in the UTM Datum WGS-84 coordinate system (World Geodetic System - 1984), compatible with the reference system SIRGAS 2000 (Geocentric Reference System of the Americas).

As a function of the diameters amplitude of the forest, 30 trees were scaled by the Smalian method, in which the heights of the stem were measured, the total heights and the diameter in the positions of 0,07 m, 0,7 m, 1,30 m, 3.3 m, 5.3 m and so on every two meters to the end of the tree. With this information, linear regression models were fitted (Table 1) for the estimation of the individual volume with bark of the stand trees.

Remotely located data

For the application of Remote Sensing techniques, an orbital image of the Landsat-8/OLI (Operational Land Imager) sensor was used, which was acquired on the United States Geological Survey platform, with the bands described in Table 2, for the date 01/30/2018, orbit 222 and point 79.

The digital processing of this image was performed in the computer application ENVI (Environment for Visualizing Images), in which the atmospheric correction was performed using the FLAASH algorithm (Fast Line-of-sight Atmospheric Analysis of Hypercubes), a process that uses physical measurements or estimates of atmospheric parameters for image correction using differential and integral equations (Gaida et al., 2020) to obtain surface reflectance. After this step, the vegetation indices were calculated, described in Table 2

Table 1. Volumetric equations tested for the estimation of the individual volume of *Pinus taeda* L.

Equation	Author
$\hat{v}= \beta_0+ \beta_1 * \boldsymbol{dbh}$	Linear
$\hat{v}= \beta_0+ \beta_1 * \boldsymbol{dbh}^2$	Kopezky-Gehrardt
$\hat{v}= \beta_0+ \beta_1 * \boldsymbol{dbh} + \beta_2 * \boldsymbol{dbh}^2$	Hohenadl-Krenn
$\hat{v}= \beta_0+ \beta_1 * \boldsymbol{dbh}^2 * H$	Spurr
$\ln \hat{v} = \beta_0+ \beta_1 * \ln dbh$	Husch
$\ln \hat{v} = \beta_0+ \beta_1 * \ln \boldsymbol{dbh} + \beta_2 * 1/dbh$	Brenac
$\ln \hat{v} = \beta_0+ \beta_1 * \ln \boldsymbol{dbh}^2 H$	Spurr
$\ln \hat{v} = \beta_0+ \beta_1 * \ln \boldsymbol{dbh} + \beta_2 * \ln H$	Schumacher-Hall

Note v: individual volume (m³); βn: model parameters; ln: natural logarithm; H: total height (m); *dbh*: diameter at 1,3 m height (cm).

Table 2. Indices of vegetation calculated for the stand of *Pinus taeda* L.

VI	Equation	Reference
ARVI	$\frac{\rho NIR - (2 * \rho RED + \rho BLUE)}{\rho NIR + (2 * \rho RED + \rho BLUE)}$	Kaufaman and Tanré (1992)
DVI	$(\rho NIR - \rho RED)$	Clevers (1988)
EVI	$2.5*(\rho NIR - B4) / (\rho NIR + 6* \rho RED - 7.5* \rho BLUE + 1)$	Gitelson et al. (1996)
EVI2	$2.5*(\rho NIR - \rho RED) / (\rho NIR + 2.4* \rho RED + 1)$	Jiang et al. (2008)
GNDVI	$\frac{\rho NIR-\rho GREEN}{\rho NIR+\rho GREEN}$	Gitelson et al. (1996)
MSAVI	$\frac{(\rho NIR-\rho RED)}{(\rho NIR-\rho RED + L)} (1+L)$	Qi et al. (1994)
MVI	$\frac{\rho NIR-\rho SWIR}{\rho NIR+\rho SWIR}$	Sousa e Ponzoni (1998)
NDVI	$\frac{\rho NIR-\rho RED}{\rho NIR+\rho RED}$	Rouse et al. (1974)
SAVI	$\frac{(1+L)\ (\rho NIR-\rho RED)}{\rho NIR + \rho RED + L}$	Huete (1988)
SR	$\frac{\rho NIR}{\rho RED}$	Jordan (1969)

Where in: VI: Vegetation Index; ARVI: Atmospherically Resistant Vegetation Index; DVI: Difference Vegetation Index; EVI: Enhanced Vegetation Index; EVI2: Enhanced Vegetation Index 2; GNDVI: Green Normalized Difference Vegetation Index; MSAVI: Modified Soil Adjusted Vegetation Index; MVI: Moisture Vegetation Index; NDVI: Normalized Difference Vegetation Index; SAVI: Soil Adjusted Vegetation Index; SR: Simple Ratio Vegetation Index; ρBLUE: Blue band reflectance; ρGREEN: Green band reflectance; ρRED: Reflectance of red band; ρNIR: Reflectance of the near Infrared band; ρSWIR: Reflectivity of the short-wave infrared band; L: constant that minimizes the effects of the soil, considered as 0.50.

With the central coordinates of the plot it was possible to perform the georeferencing of the same in the image. Using the buffer tool, available in a GIS environment, an area of equal radius of the plot (11.28 meters) was constructed around the central point of each plot. Finally, the average value of each vegetation index per plot was obtained with the Zonal Statistics as a Table tool in a GIS environment (Esri, 2018).

With these data, a Pearson correlation analysis was performed between the dendrometric variables per plot (volume and basal area) (m^3/0.04ha) with the mean vegetation indices per plot. The indices better correlated with these parameters were used in the construction of regression models by the Stepwise technique. For this, the dependent variables comprised the forest parameters and the independent variables involved the vegetation indexes. The adjusted regression models are shown in Table 3.

Table 3. Regression models adjusted for volume and basal area estimation by plot (m^3 0.04ha^{-1}) using vegetation indices from Landsat-8.

	Volume by plot (m^3 0,04ha^{-1})	
Model	**Equation**	**Author**
1	$V= \beta0 * IV^{\beta1} + \varepsilon$	Berkhout
2	$V= \beta0 * \beta1 * \frac{1}{IV} + \varepsilon$	Curtis
3	$V= \beta1 * IV + \beta2 * IV^2 + \varepsilon$	Dissescu-Meyer
4	$V= \beta0 + \beta1 * IV + \beta2 * IV^2 + \varepsilon$	Hohenadl-Krenm
5	$V= \beta0 + \beta1 * IV^2 + \varepsilon$	Kopezky-Gehrardt
6	$V = \beta_0 + \beta_1 * IV + \beta_2 * IV2 + \beta_3 IV^2 + \beta_4 * IV^3 + \beta_5 * IV^4 + \beta_6 * IV^5 + \beta_7 * IV2^2 + \beta_8 * IV * IV2 + \beta_9 * \ln IV * \ln IV2 + \beta_{10} * \frac{1}{IV^3} * 1/IV2$	Stepwise 1
7	$V = \beta_0 + \beta_1 * IV + \beta_2 * IV2 + \beta_3 IV^2 + \beta_4 * IV^3 + \beta_5 * IV^4 + \beta_6 * IV^5 + \beta_7 * IV2^2 + \beta_8 * IV2^3 + \beta_9 * \frac{1}{IV^2} + \beta_{10} * IV * IV2 + \beta_{11} * \frac{1}{IV^3} * 1/IV2$	Stepwise 2
	Basal area by plot (m^2 0,04ha^{-1})	
1	$G = \beta0 * IV^{\beta1} + \varepsilon$	Berkhout
2	$G = \beta0 * \beta1 * \frac{1}{IV} + \varepsilon$	Curtis
3	$G = \beta1 * IV + \beta2 * IV^2 + \varepsilon$	Dissescu-Meyer
4	$G= \beta0 + \beta1 * IV + \beta2 * IV^2 + \varepsilon$	Hohenadl-Krenm
5	$G = \beta0 + \beta1 * IV^2 + \varepsilon$	Kopezky-Gehrardt
6	$G = \beta_0 + \beta_1 * IV^2 + \beta_2 * IV^3 + \beta_3 IV^4 + \beta_4 * IV^5 + \beta_5 + IV2^3 + \beta_6 + * IV2^5 + \beta_7 * \ln IV^2 + \beta_8 EXP\ IV^4 + \beta_9 * EXP + \beta_{10} * \frac{1}{IV2^3} * 1/IV$	Stepwise 1
7	$G = \beta_0 + \beta_1 * IV^2 + \beta_2 * IV^3 + \beta_3 * IV^4 + \beta_4 * IV^5 + \beta_5 * IV2^2 + \beta_6 * IV2^3 + \beta_7 * IV2^5 + \beta_8 * \ln IV + \beta_9 * EXP\ IV + \beta_{10} * EXP\ IV^4 + \beta_{10} * \frac{1}{IV^3} * 1/IV2 + \beta_{11} * \frac{1}{IV2^3} * 1/IV$	Stepwise 2

Note: V: volume by plot (m^3 0.04ha^{-1}); G: basal area by plot (m^2 0.04ha^{-1}); βi: parameters to be estimated; IV: vegetation index (indicated by correlation analysis); IV2: vegetation index 2 (indicated by correlation analysis); ε: error associated with the model.

It is noteworthy that the models for estimating basal area and volume per unit area are adaptations of individual tree volume models.

Model selection

The selection of the best model was performed considering the statistical criteria: adjusted coefficient of determination (R^2 aj.) (Equation 2), standard error of the estimate (Equation 3) and standard error of the estimate, in percentage (Syx%) (Equation 4) according to Moeser and Oliveira (2011). In addition to these factors, the graphical analysis of the residues was also evaluated.

$$R^2 = \frac{SQ_{reg}}{SQ_{tot}} \quad (1)$$

$$R^2aj = 1-\left\{ \left(1-R^2\right)* \left(\frac{n-1}{n-p}\right)\right\} \quad (2)$$

$$Syx = \sqrt{\frac{\sum (y-yi)^2}{n-p}} \quad (3)$$

$$Syx = \frac{Syx}{\hat{Y}} *100 \quad (4)$$

Note: R^2: coefficient of determination; SQreg: Sum of regression squares; SQtot: sum of squares total; R^2 aj: adjusted coefficient of determination; n: number of trees that were planted; p: number of parameters of the equation; Syx: standard error of the estimate (m^3); yi: observed volume (m^3); yi: estimated volume (m^3); Syx (%): standard error of the estimate in percentage (%); $\hat{Y}$: mean of observed values (m^3).

In addition, other fit metrics were evaluated: Akaike Information Criterion (AIC) and Bayesian Information Criterion (BIC). The first one reflects the loss of information associated with the predictions of a model and the observed values. Thus, the lower the AIC, the more explanatory the model (Moser and Oliveira, 2011). The AIC was obtained by Equation 5:

$$AIC = 2 \log (\theta) + 2k \quad (5)$$

Note: $\log L(\theta)$: logarithm of the maximum likelihood function; k: number of model parameters.

The BIC also increases with the sum of squares of the residues and the smaller the value, the better the model. Equation 6 obtained this criterion:

$$BIC = -2 \log (L_p) + [(p+1)+1] \log (n) \quad (6)$$

Note: n: number of observations in the sample; p: number of model parameters; Lp: maximum likelihood function of the model.

The Root Mean Squared Error (RMSE) (Equation 7) was also calculated and evaluates the differences between the observed values and the values predicted by the regression model (Moser and Oliveira, 2011):

$$RMSE = \sqrt{\frac{\sum (y - yi)^2}{n}} \quad (7)$$

Where in: RMSE: Root Mean Square Error; y: observed volume; yi: estimated volume; n: number of observations.

The best method was determined by the metrics previously mentioned (Equation 2, 3, 4, 5, 6 and 7). The fit of the models and calculations of the adjustment metrics were developed in software R version 3.4.1. (R CORE TEAM, 2018).

Results and Discussion

Individual volume models

The adjustment of the regression models for estimating the individual volume with bark of the stand trees (Figure 2) revealed regular statistics, with R^2 adjusted between 0.9192 to 0.9954 and standard error of the estimate between 7.69 and 27.69%. The best adjusted model for the stand of *Pinus taeda* L. was the logarithmized Spurr model (Spurr log), due to the higher adjusted R^2 (0.9954), lower error (7.69%) and better distribution of residues (Figure 2).

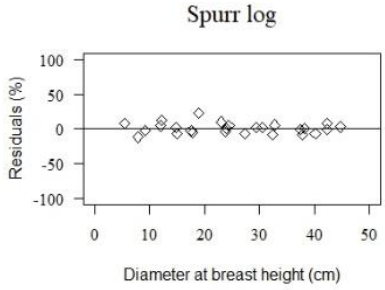

Figure 2. Graphical distribution of the residuals for the best fitted regression models for the individual volume estimation of the trees of the stand of *Pinus taeda* L.

Correlation analysis

The correlation of vegetation indexes with basal area (Table 4) showed that there was a negative and positive correlation, and the highest correlation was observed in the MVI index, with 0.51. For the other indexes, the correlation ranged from -0.12 to 0.43. As for the correlation between vegetation index and volume (Table 5), the highest correlation was with the GNDVI index, with 0.47.

The values of the correlation between basal area and volume (Table 4 and 5) with vegetation indices can be explained by the bands used in the calculation of vegetation indices obtained. The negative correlations found are related to the amount of shadow effects and the amount of dots in the area that have the highest brightness. These points increase as the volume and age of the trees increase, which causes a reduction in spectral response (Franklin et al., 2001).

Table 4. Pearson correlation coefficients between basal area per plot and the mean vegetation indexes per plot obtained with Landsat-8.

	G
G	1
ARVI	0,31
DVI	0,18
EVI	-0,12
EVI2	0,40
GNDVI	0,35
MSAVI	0,40
MVI	0,51*
NDVI	0,43
SAVI	0,40
SR	0,43

Note: G: basal área by plot (m^2 0.04ha^{-1}).
* Significant correlation at 5% probability.

Table 5. Pearson correlation coefficients between volume per plot and the mean vegetation indexes per plot obtained with Landsat-8.

	V
V	1
ARVI	0,21
DVI	0,09
EVI	-0,03
EVI2	0,33
GNDVI	0,47*
MSAVI	0,33
MVI	0,40
NDVI	0,36
SAVI	0,33
SR	0,36

Note: V: volume by plot (m^3 0.04ha^{-1}).
* Significant correlation at 5% probability.

Spanner et al. (1990) states that closed dents have positive correlations and negative correlations are found in areas with open canopies. The population in question has large open areas, due to thinnings carried out, which may have directly influenced the band reflectance, and consequently the indexes obtained and its correlation with the variables.

For the basal area, the best correlated index was the MVI, whose equation is formed by the ratio between the near-infrared and short-wave infrared bands. The reflectance in the near infrared spectral range is caused by the internal structure of the sheet. Thus, if there are more internal spaces in the internal structure of the leaf, the greater the reflectance in this range. In this study, it was observed that the canopy cover and the growth of the trees caused an increase in the reflectance in the near infrared (Ponzoni et al., 2012). In shortwave infrared, the reflectance of the leaves decreases due to strong bands of water absorption.

The highest correlation observed for the volume was with the GNDVI index, which in turn, presents the substitution of the red band by the green band in its formula. The spectral behavior of these bands shows that there is a negative linear correlation between the reflectance factor and the green vegetation in the red wavelength. In the near infrared, this correlation is positive.

Berra et al. (2016) also list characteristics of the stands as height, type of management and relief of the area as factors that may have influenced the relationship between vegetation indexes and the variables basal area and volume. In that study, age and the type of management were important factors in the relationship of spectral bands to the volume of wood stand.

Estimation of forest parameters using SR

The fit of the regression models for the estimation of basal area per plot (Table 6) from the IV with the highest correlation revealed statistics with low to moderate precision. The first model was not adjustable. The models 2, 4, 5 and 6 showed low R^2 adjusted and, consequently, bigger errors. Only model 3 and 6 had satisfactory fitting metrics.

Table 6. Adjustment statistics of the regression models tested for Landsat-8 sensors to estimate basal area per plot (m^2 0.04ha^{-1}) using vegetation indexes.

Model	R^2 aj	Syx	Syx (%)	AIC	BIC	F	RMSE
1	-	-	-	-	-	-	-
2	0,0191	0,27	17,02	9,425	12,41	1,372	0,26
3	0,9156	0,27	17,08	10,31	12,63	342,49	0,26
4	-0,0374	0,28	17,52	11,40	15,38	0,657	0,26
5	0,0202	0,27	17,07	9,41	12,39	1,392	0,26
6	0,5213	0,1941	11,93	-1,869	12,31	2,724	0,11
7	0,0449	0,5316	32,67	39,52	49,48	1,112	0,39

Note: R^2 aj: adjusted determination coefficient; Syx: standard error of the estimate (m^3 0.04ha^{-1}); Syx (%): standard error of the estimate in percentage; AIC: Akaike Information Criteria; BIC: Bayesian Information Criterion; F: significance test at 5% probability; RMSE: Root Mean Square Error (m^3 0.04ha^{-1}).

Table 7. Adjustment statistics of the regression models tested for Landsat-8 sensors to estimate volume per plot (m^3 0.04ha-^{1}) using vegetation indexes.

Model	R^2 aj	Syx	Syx (%)	AIC	BIC	F	RMSE
1	0,4855	3,95	18,11	115,59	118,57	-	3,75
2	0,1525	4,04	18,56	116,57	119,56	4,420	3,84
3	0,9143	3,95	18,15	121,45	134,72	306,274	3,75
4	0,3409	3,56	16,37	112,40	116,38	5,915	3,29
5	0,1873	3,96	18,17	115,74	118,75	5,379	3,76
6	0,5639	2,90	13,31	107,42	119,38	3,457	1,94
7	0,4076	3,38	15,55	111,44	126,37	2,006	1,85

Note: Model: model a 1 7 were derived from the Stepwise technique model; R^2 aj: adjusted determination coefficient; Syx: standard error of the estimate (m^3 0.04ha-^{1}); Syx (%): standard error of the estimate in percentage; AIC: Akaike Information Criteria; BIC: Bayesian Information Criterion; F: significance test at 5% probability; RMSE: Root Mean Square Error (m^3 0.04ha^{-1}).

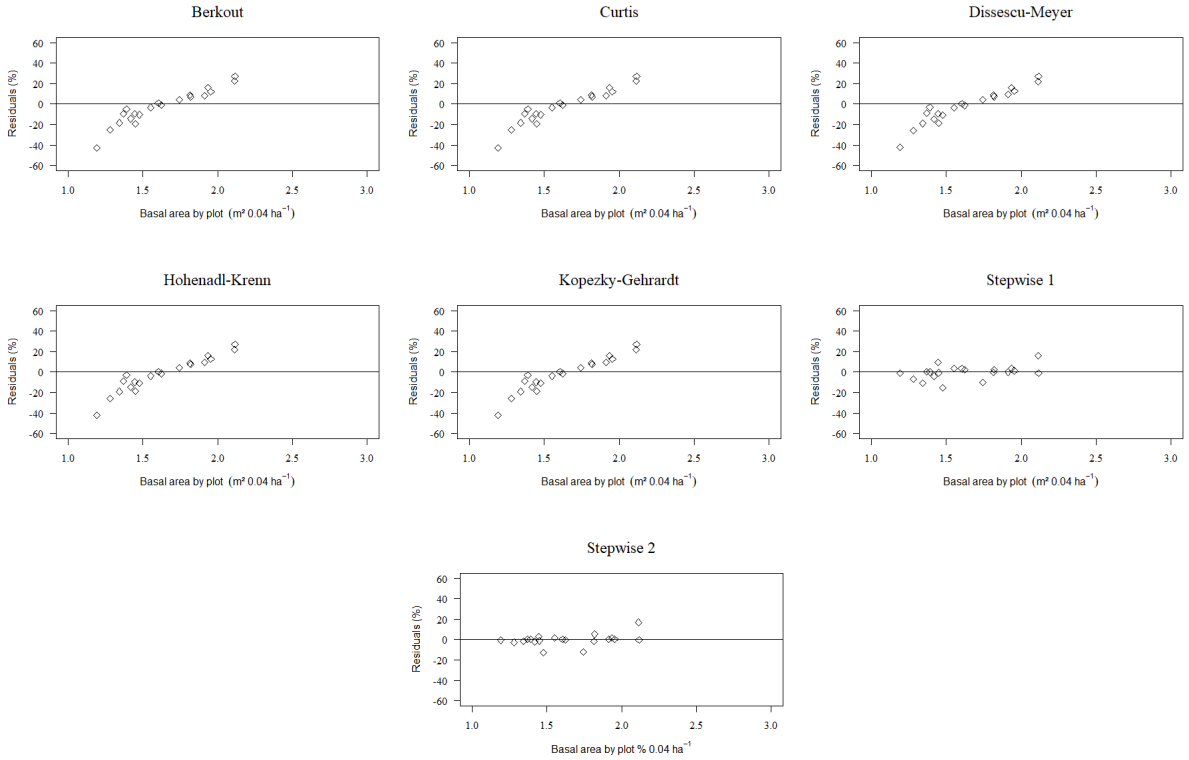

Figure 3. Graphical dispersion of the residuals of the models adjusted with the Landsat-8 data in the estimation of basal area per plot (m^2 0.04 ha^{-1}) of a stand of *Pinus taeda* L.

Table 7 illustrates the model adjustment metrics for volumetric prediction per plot, revealing that the volumetric regression models were higher than the basal area as a function of the higher adjusted R^2 and the smaller standard error of the estimate (Table 6).

In the graphical analysis of the residuals for the regression models for basal area (Figure 3) it is possible to notice that in the model 6 (Stepwise 1) there was a more concentrated distribution around the regression line. In the other models, the residues presented similar behavior, with the presence of outliers, underestimates, and super estimates.

Among the models tested for the estimation of basal area per plot, the model generated by the Stepwise 1 technique can be indicated as the most adequate to estimate this variable using vegetation indices, due to the higher adjusted R^2, lower error and better graphic distribution waste.

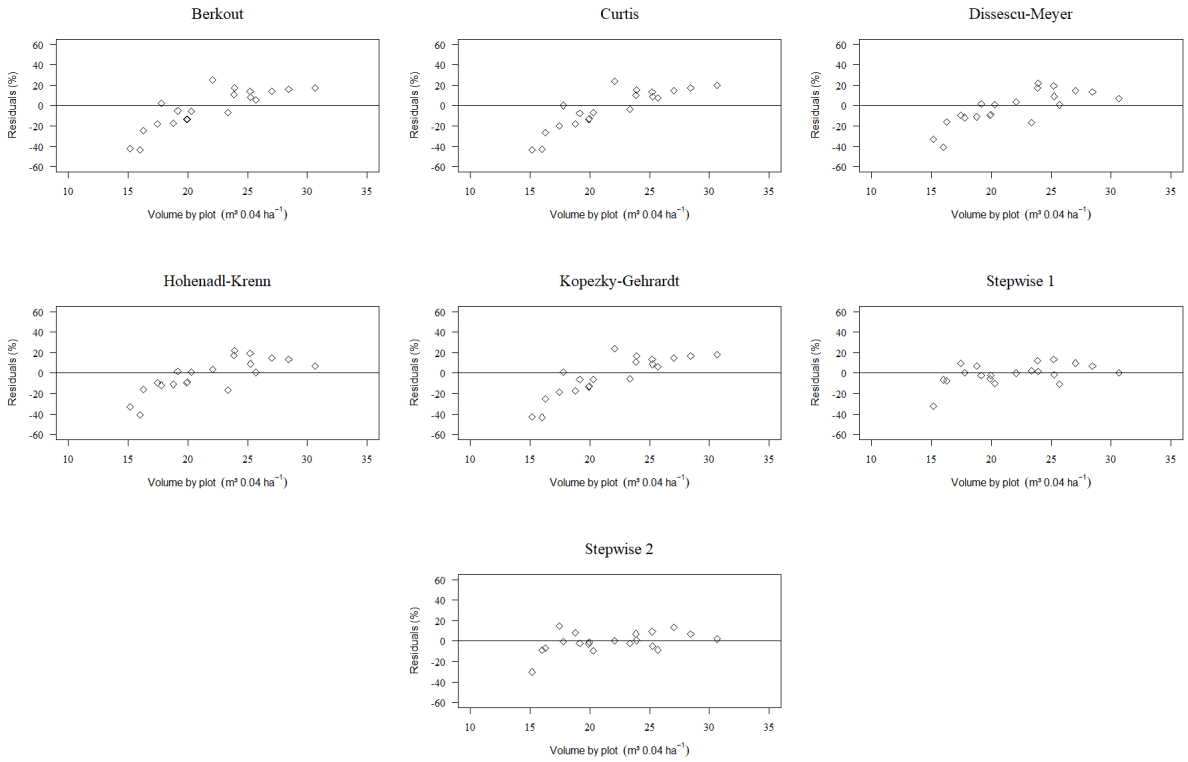

Figure 4. Graphical dispersion of the residuals of the models adjusted with the Landsat-8 data in the volume estimate per plot (m^3 0.04 ha^{-1}) of a stand of *Pinus taeda* L.

For the residuals of the fitted volumetric models (Figure 4), a similar behavior of the residues can be observed in observed in two of all the adjusted models. It is possible to notice the absence of independence of the errors, one of the assumptions of the regression analysis in all the models. In addition, there were underestimates and over estimates, as well as the presence of outliers. However, the model that presented the best volume estimate as a function of the best vegetation indices correlated to the Landsat-8 data was the first model generated by the Stepwise technique, due to the higher coefficient of determination adjusted (0.9143) and lower standard error of the estimate (13.31%) and the best graphical distribution of the residues.

The quality of the fitted models for basal area and volume estimation is directly related to the obtained vegetation index values. It is worth mentioning the existing constraints on the association between remotely located data and forest inventory data. Meng et al. (2007) state that the inclusion of characteristics such as geology, climate, soil effects and site index of the stand in the fit of the models would favor the accuracy of the estimates. Another important detail concerns the size and the identification of the plots, because in this study, the size of the plots was inferior to the spatial resolution of the Landsat-8 sensor (30 m) and the identification of the plots with the View Ranger application also resulted in errors of location up to 10 meters from field plots, caused by the closure of the forest canopy.

The sensors of the Landsat constellation have already been used in other researches for the quantification of forest parameters, such as basal area and volume, as the studies cited below.

The volume of a stand of Pinus elliotti Engelm. from Landsat-5 TM and LISS-III/ResourceSat-1 data was estimated by Berra et al. (2016). The linear correlation of Landsat-5 data was lower than that obtained with LISS-III. However, reflectance values in four spectral ranges (blue, green, red and infrared) were equivalent for the two sensors that represented sensitivity to the volumetric potential changes of the area, indicating the possibility of integration between LISS and TM images for such surveys.

The identification of commercial Eucalyptus grandis plantations of different ages and the estimation of total wood volume of these areas using Landsat-8/OLI sensor images was performed by Alba et al. (2017). The data remotely allowed the differentiation of the stages of growth of the species in question and the estimate of the volume through the SAVI index, which better represented the changes in the volume of the stand. The selection of variables by the Stepwise method generated adjusted models with R^2 adjusted above 0.70 and standard error of the estimate of 60.08 m^3 ha^{-1}.

The evaluation of the seasonal data of Landsat-8/OLI satellite images in the estimation of

the variables tree density, basal area and volume of wood of a heterogeneous forest in the Mediterranean in the northeast of Greece was done by Chrysafis et al. (2017). The results revealed that the selection of variables to reduce the number of predictor variables improved the prediction accuracy of all three attributes. The R^2 of the models was 0.541 for the density of trees, 0.724 for basal area and 0.68 for volume considering the dry season. The model generated from a multi temporal image generated R^2 of 0.532 for tree density, 0.716 for basal area and 0.653 for volume.

Santos et al. (2017) tested the feasibility of the use of multispectral images of the Landsat-8/OLI sensor through regression analysis with field data, for the estimation of forest parameters in the Cerrado area. For the volume, the adjusted R^2 ranged from 0.40 to 0.49. For the basal area, the adjusted R^2 of the models ranged from 0.61 to 0.66. The authors concluded that this methodology presents application potential in Cerrado areas and that NDVI presented the best correlation with the estimated variables.

The estimation of forest attributes by a combination of Landsat-8/OLI sensor images and forest inventory data by the kNN (k Nearest Neighbor) method as a non-parametric method was tested by Abedi et al. (2018). The data demonstrated that the use of kNN was satisfactory in the basal area estimation, but it has less efficiency to estimate tree density and volume.

Another factor that had great influence on the obtained results was the spatial resolution of the sensor tested. The use of high spatial resolution sensors could contribute to the improvement of estimates of dendrometric variables.

Dalponte et al. (2018) evaluated models for predicting above-ground biomass and their combination with airborne SR data for DBH and biomass predictions at plot level in boreal forests using remotely detected data from Airborne Laser Scanner (ALS) and hyperspectral data. The comparison among models developed in field data versus models developed from remote sensing data revealed that both can be used in predicting the variables; however, there was a large systematic error. Because of this, the authors suggest caution in the use of these models.

Acknowledgments

The authors would like to thank the FAPESC research funding agency (Foundation for Support for Research and Innovation in the State of Santa Catarina) to the Forest Resources Management research group.

Conclusions

The vegetation index that presented the best correlation with the basal area was the MVI and for the volume the GNDVI. It was possible to estimate basal area and stand volume through remotely located data. Regarding modeling, it was possible to notice the superior performance of Stepwise techniques when compared to traditional modeling techniques.

References

Abedi R, Bonyad AE, Moridani AY, Shahbahrami A (2018) Evaluation of IRS and Landsat 8 OLI imagery data for estimation forest attributes using k nearest neighbour non-parametric method. *International Journal of Image and Data Fusion*, 15. DOI: 10.1080/19479832.2018.1440439.

Alba E, Marchesan J, Mello EP, Tramontina J, Silva EA, Pereira RS (2017) Uso de imagens de média resolução espacial para o monitoramento de dosséis de Eucalyptus grandis. *Revista Scientia Agraria*, Curitiba, 18(4):01-08. doi:10.5380/rsa.v18i4.51944

Alrababah MA, Alhamad MN, Bataineh AL, Bataineh MM, Suwaileh AF (2011) Estimating east Mediterranean forest parameters using Landsat ETM, *International Journal of Remote Sensing*, 32:6,1561-1574.DOI: 10.1080/01431160903573235

Almeida AQD, Ribeiro A, Delgado RC, Rody YP, Oliveira ASD, Leite FP (2015) Índice de área foliar de Eucalyptus spp. estimado por índices de vegetação utilizando Imagens TM – Landsat-5. *Floresta e Ambiente*, 22(3):368-376. doi: 10.1590/2179-8087.103414.

Alvares CA, Stape JL, Sentelhas PC, Gonçalves JLM, Sparovek G (2013) Köppen's climate classification map for Brazil. *Meteorologische Zeitschrift*, 22 (6):711-728. doi: 10.1127/0941-2948/2013/0507.

Assmann E (1970) *The principles of forest yield study*. New York: Pergamon Press, 506p.

Berra EF, Brandelero C, Pereira RS, Sebem E, Goergen LCG, Benedetti, ACP, Lippert DB (2012) Estimativa do volume total de madeira em espécies de eucalipto a partir de imagens de satélite Landsat. *Ciência Florestal*, Santa Maria, 22(4):853-864.

Berra EF, Fontana DC, Kuplich TM (2016) Comparison of satellite imagery from LISS-III/Resourcesat-1 and TM/ Landsat 5 to estimate stand-level timber volume. *Pesquisa Florestal*

Brasileira, Colombo, 36(88):363-373. doi: 10.4336/2016.pfb.36.88.1134

Chinembiri T, Bronsveld M, Rossiter D, Dube T (2013) The precision of C stock estimation in the Ludhikola watershed using model-based and design-based approaches. *Natural Resources Research*, 22(4):297–309. DOI: 10.1007/s11053-013-9216-6

Chrysafis I, Mallinis G, Gitas I, Tsakiri-strati M (2017) Estimating Mediterranean forest parameters using multi seasonal Landsat 8 OLI imagery and an ensemble learning method. *Remote Sensing of Environment*, 199:154-166. DOI: 10.1016/j.rse.2017.07.018

Clevers JGPW (1988) The derivation of a simplified reflectance model for the estimation of Leaf Area Index. *Remote Sensing Environment*, 25: 53-69.

Dube T, Mutanga O, Abdel-Rahman EM, Ismail R, Slotow R (2015) Predicting *Eucalyptus* spp. stand volume in Zululand, South Africa: an analysis using a stochastic gradient boosting regression ensemble with multi-source data sets. *International Journal Remote Sensing*, 36(14):3751–3772. DOI: 10.1080/01431161.2015.1070316

Esri (2018). Environmental Systems Research Institute. ArcGIS Professional GIS for the desktop, version 10.4.1. Disponível em: https://support.esri.com/en/Products/Desktop/arcgis-desktop/arcmap/10-4-1. Acesso em: 20 abr. 2018.

Gaida W, Breuning FM, Galvão, LS, Ponzoni FJ (2020) Correção Atmosférica em Sensoriamento Remoto: Uma Revisão. *Revista Brasileira de Geografia Física*, 13(1):229-248.

Gara TW, Murwira A, Chivhenge E, Dube T, Bangira T, (2014) Estimating wood volume from canopy area in deciduous woodlands of Zimbabwe. Southern Forests: *Journal Forest Science*, 76(4):237–244. DOI: 10.2989/20702620.2014.965981

Gao BC (1996) NDWI a normalized difference water index for remote sensing of vegetation liquid water from space. *Remote Sensing of Environment*, New York, 58:257-266.

Gitelson AA, Kaufman YJ, Merzlyak MN (1996) Use of a green channel in remote sensing of global vegetation from EOS-MODIS. *Remote Sensing of Environment*, New York, 58:289-298. DOI: 10.1016/S0034-4257(96)00072-7

Gunlu A, Ercanli I, Sönmez T, Başkent EZ (2014) Prediction of some stand parameters using pansharpened IKONOS satellite image. *European Journal of Remote Sensing*, 47:329-342. DOI: 10.5721/EuJRS20144720

Franklin SE (2001) Remote Sensing for Sustainable Forest Management (Boca Raton, FL: CRC Press).
Huete AR (1988) A soil-adjusted vegetation index (SAVI). *Remote Sensing of Environment*, New York, 25(3):295-309.

Huete AR, Liu HQ, Leeuwen, WV (1997) A comparison of vegetation indices over a global set of TM images for EOS-MODIS. *Remote Sensing of Environment*, New York, 59:440-451. DOI: 10.1016/S0034-4257(96)00112-5

Jiang Z, Huete AR, Didan K, Miura T (2008) Development of a two-band enhanced vegetation index without a blue band. *Remote Sensing of Environment*, New York, 112: 3833-3845. DOI: 10.1016/j.rse.2008.06.006

Jordan CF (1969) Derivation of leaf area index from quality of light on the forest floor. *Ecology*, 50:663-666. DOI: 10.2307/1936256.

Kaufman YJ, Tanré D (1992) Atmospherically resistant vegetation index (ARVI) for EOS-MODIS. *IEEE Transactions on Geoscience and Remote Sensing*, 30:261-270. DOI: 10.1109/36.134076.

Mallinis, G., N. Koutsias, A. Makras, and M. Karteris (2004) Forest Parameters Estimation in a European Mediterranean Landscape Using Remotely Sensed Data. *Forest Science*, 50: 450–460.

Meng Q, Ceiszewski CJ, Madden M, Bordes B (2007) A linear mixed-effects model of biomass and volume of trees using Landsat ETM+ images. *Forest Ecology and Management*, Amsterdam, 244(3):93–101. DOI: 10.1016/j.foreco.2007.03.056

Moser P, Oliveira LZ (2017) *Regressão linear aplicada à dendrometria:* uma introdução e iniciação à linguagem R. Blumenau: Edifurb,152p.

Ponzoni FJ, Shimabukuro YE, Kuplich TM (2012) *Sensoriamento remoto aplicado ao estudo da vegetação*. 2.ed. atual. e ampl. São Paulo: Oficina de Textos, 160p.

Qi J, Chehbouni A, Huete AR, Kerr YH, Sorooshian S (1994) A modified soil adjusted vegetation index. *Remote Sensing of Enviroment*, 48: 119-126.

R core team. R: A language and environment for statistical computing. R Foundation for Statistical Computing, Vienna, Austria. Disponível em: <https://www.R-project.org/>. Acesso em 16/02/2018.

Richardson AI, Wegand CL (1977) Distinguishing vegetation from soil background information. *Photogrammetric Engineering and Remote Sensing*, Bethesda, 43(12):1541-1552.

Rouse JWRH, Haas JA, Schell DWD (1974) Monitoring vegetation systems in the Great Plains with ERTS, In: S.C. Freden, E.P. Mercanti, and M. Becker (eds) Third Earth Resources Technology Satellite–1 Syposium. Volume I: Technical Presentations, NASA SP-351, NASA, Washington, D.C., pp. 309-317.

Santos MM, Machado IES, Carvalho EV, Viola MR, Giongo M (2017) Estimativa de parâmetros florestais em área de cerrado a partir de imagens do sensor OLI Landsat 8. *Floresta*, Curitiba, 47(1):75-83. DOI: 10.5380/rf.v47i1.47988

Sousa CL, Ponzoni FJ (1998) *Avaliação de índices de vegetação e de bandas TM/LANDSAT para estimativa de volume de madeira em floresta implantada de Pinus spp*. In: Simpósio Brasileiro de Sensoriamento Remoto, 9., 1998. Santos. Anais... Santos, SBSR, 1998.

Spanner MA, Pierce LL, Peterson DL, Running SW (1990). Remote Sensing temperate coniferous forest leaf area index: the influence of canopy closure, understory and background reflectance. *International Journal of Remote Sensing*, London, 11(1):95-111. DOI: 10.1080/01431169008955002

Stournara P, Patias P, Karamanolis D (2017) Evaluating wood volume estimates derived from Quickbird imagery with GEOBIA for Pinus nigra trees in the Pentalofo forest, northern Greece. *Remote Sensing Letters*, 8, 96–105.

Tesfamichael S, Van Aardt J, Ahmed F (2010) Estimating plot-level tree height and volume of Eucalyptus grandis plantations using small-footprint, discrete return LiDAR data. *Progress in Physical Geography*, 34(4):515–540. DOI: 10.1177/0309133310365596

Zhang Y, Guanter L, Berry JA, Joiner J, Van Der Tol C, Huete A, Gitelson A, Voigt M, Köhler P. Estimation of vegetation photosynthetic capacity from space-based measurements of chlorophyll fluorescence for terrestrial biosphere models. *Global Chang Biology*, 20:3727-3742. DOI: 10.1111/gcb.12664.